Di-, Tri-, and Tetranuclear Complexes of Ni, Pd, and Zn with Oxalamidinato Bridges: Syntheses, Structures and Catalytic Reactions

Dirk Walther,*[a] Thomas Döhler,[a] Nils Theyssen,[a] and Helmar Görls[a]

Keywords: Nickel / N ligands / Oligomerizations / Palladium / Polymerizations

The reaction of oxalic amidines $R^1N{=}C(NHR^2){-}C(NHR^2){=}NR^1$ ($oxamH_2$) with 2 equiv. $(allyl)_2M$ or $(acac)_2M$ (M: Ni, Pd) results in the formation of dinuclear complexes [(**T**)M(oxam)M(**T**)] containing dianionic bridging oxalamidinate and η^3-allyl or acac as terminal ligands **T**. The complexes were characterized by elemental analyses, mass spectrometry, and ^1H and ^{13}C NMR spectroscopy. In addition, the solid-state structures of **1** (M: Ni; **T**: η^3-allyl; R^1 = *p*-tolyl; R^2 = mesityl), **2** (M: Ni; **T**: η^3-allyl; $R^1 = R^2$ = mesityl), **9** (M: Pd; **T**: acac; R^1 = phenyl; R^2 = *p*-tolyl), and **10** (M: Pd; **T**: acac; $R^1 = R^2$ = *p*-tolyl) were determined by X-ray single-crystal diffraction analyses. All complexes contain the metal ions in a square-planar environment. Furthermore, in the η^3-allyl complexes two isomers are found in which the two allyl groups are oriented in *syn* and *anti* positions. Trinuclear complexes of the composition [(**T**)M(oxam)M^1(oxam)M(**T**)] (M^1: Zn; M: Ni or Pd) are obtained by treating Et_2Zn with 2 equiv. of an oxalic amidine in toluene, followed by addition of 2 equiv. $M(acac)_2$ or $Pd(allyl)_2$. The synthesis and solid-state X-ray analysis of the tetranuclear complex [(**T**)M(oxam)M^1(oxam)M^1(oxam)M(**T**)] (**16**: M = M^1: Zn; oxam: R^1 = *p*-tolyl; R^2 = mesityl) is also described. A number of Ni^{II} complexes oligomerize or polymerize ethylene upon activation with MAO or Et_3Al. The catalyses can be adjusted by the bulkiness of the nitrogen substituents, the nature of the cocatalyst, and the nuclearity of the complexes. The most active and selective polymerization catalyst is the heterotrinuclear NiZnNi complex **12** which contains two tetramesityloxalamidinato bridges and acac as terminal ligands **T**. Complex **12** can be activated by using only 2 equiv. Et_3Al per Ni. Initial efforts show that the palladium complexes are catalysts for the Heck coupling.

Introduction

Transition metal complexes with oxalic acid amidinato bridging ligands (“oxam“) have, surprisingly, attracted little attention. Complexes of this type should be interesting candidates for a number of attractive applications, such as the construction of well-defined linear oligonuclear complexes or the synthesis of coordination polymers starting from dinuclear complexes which contain labile terminal ligands **T**. Moreover, linear oligometal complexes with tuneable catalytic properties at peripheral positions, adjusted by inner metal ions, should offer new possibilities for catalytic reactions.

Since oxalamidinato complexes have the tendency to form ill-defined polymeric amorphous complexes[1,2] only a few structurally characterized complexes are known. The first dinuclear complex $Cp_2Ti(oxam)TiCp_2$ has been synthesized by Floriani in the 1970s.[3] Döring and Beckert prepared a number of mono- and dinuclear complexes containing for example $M(CO)_4-$ and/or the Cp_2Ti- fragments and investigated the organic chemistry of these complexes.[4−7]

We have found that mono- and dinuclear ruthenium complexes containing bpy derivatives as additional supporting ligands form stable compounds which are non-luminescent.[8] Furthermore, we have prepared the first example of dinuclear magnesium oxalamidinates. These compounds reacted with carbon dioxide to form trimeric carbamato complexes which can be considered as structural models for rubisco.[9]

In a preliminary paper we have recently communicated that dinuclear nickel complexes of the type [(acac)Ni(oxam)-Ni(acac)] can readily be synthesized by treating free oxalic amidines with $Ni(acac)_2$. Additionally, the first linear tri- and tetranuclear complexes could be isolated.[10] Some of the complexes were found to be catalytically active in ethylene oligomerization or polymerization upon activation with MAO. Apart from our preliminary communication there exists no report of oxalamidinato complexes having been used in catalytic C−C linkage reactions. From a general point of view we can consider oxalic amidinato complexes as members of a general range of the following composition in which each oxam ligand bridges two metal fragments.

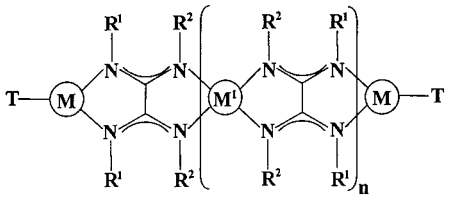

In this paper we describe the construction of well-defined di- or oligometal Ni, Pd, and Zn complexes of the above range, and investigate their catalytic behaviour in the oligomerization/polymerization of ethylene. Furthermore, initial

[a] Institut für Anorganische und Analytische Chemie der Universität Jena,
August-Bebel-Straße 2, 07743 Jena, Germany

  1434−1948/01/0808−2049 $ 17.50+.50/0

investigations of the use of some of the complexes in the Heck coupling are communicated.

Results and Discussion

Dinuclear Complexes Containing Ni, Pd, or Zn

Table 1 shows the dinuclear complexes **1**−**11** containing η^3-allyl or acetylacetonato ligands as terminal groups which were used in both the catalytic ethylene conversion and as catalysts in the Heck reaction. Complexes **6**−**8** were already described in a preliminary paper.[10]

Table 1. Di- and trinuclear oxalamidinato complexes (according to Schemes 1 and 3)

Compd.	M	Terminal ligand **T**	R^1	R^2
Dinuclear complexes of the type (**T**)M(oxam)M(**T**)				
1	Ni	η^3-allyl	*p*-tolyl[a]	mesityl[a]
2	Ni	η^3-allyl	mesityl	mesityl
3	Pd	η^3-allyl	phenyl	*p*-tolyl
4	Pd	η^3-allyl	*p*-tolyl	*p*-tolyl
5	Pd	η^3-allyl	*p*-tolyl	mesityl
6	Ni[10]	acac	*p*-tolyl	*p*-tolyl
7	Ni[10]	acac	*p*-tolyl[b]	mesityl[b]
8	Ni[10]	acac	mesityl	mesityl
9	Pd	acac	phenyl[c]	*p*-tolyl[c]
10	Pd	acac	*p*-tolyl	*p*-tolyl
11	Ni/Zn	acac	mesityl	mesityl
Trinuclear complexes of the type (**T**)M(oxam)Zn(oxam)M(**T**)				
12	Ni	acac	mesityl	mesityl
13	Pd	acac	*p*-tolyl	*p*-tolyl
14	Pd	η^3-allyl	*p*-tolyl	*p*-tolyl

[a] (*E*) arrangement of R^1 and R^2 (Scheme 2, **A** and **B**). − [b] (*Z*) arrangement of R^1 and R^2 (Scheme 2, **C** with acac instead of allyl). − [c] (*E*) arrangement of R^1 and R^2 (Scheme 2, **A** with acac instead of allyl).

A variety of dinuclear η^3-allyl complexes of Ni^{II} and Pd^{II} could be prepared by the reaction of the corresponding bis(η^3-allyl)metal complexes with the oxalic amidine (molar ratio 2:1, Scheme 1). In these reactions propene was eliminated resulting in neutral complexes of the type [(allyl)M-(oxam)M(allyl)] which are the first members of the above-mentioned homologous range (with $n = 0$).

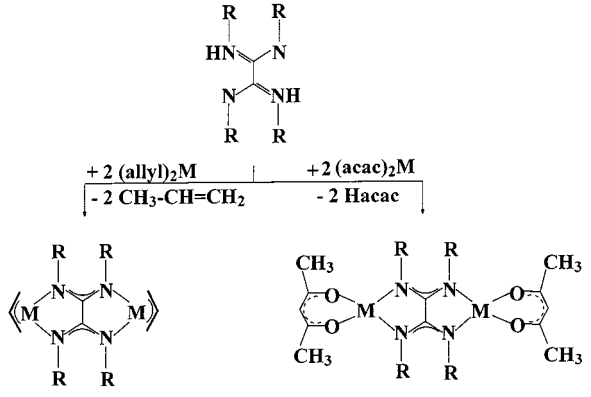

Scheme 1. Syntheses of dinuclear complexes **1**−**10**

Analogous dinuclear oxalamidinato complexes **6**−**10** containing acetylacetonato groups as terminal ligands were obtained in good yields starting from the corresponding bis(acetylacetonato)metal(II) complexes and oxalamidines (molar ratio 2:1). After workup, complexes of the type [(acac)M(oxam)M(acac)] (**6**−**10**) were isolated as crystalline compounds. The formation of coordination polymers was not observed in this reaction, due to the stable bonding of the terminal acetylacetonates in **6**−**10**. On the other hand, the complexes can easily react with organoaluminium compounds to form dinuclear Ziegler−Natta catalysts.

The synthesis of the heterodinuclear compound **11** required another preparative route: Reaction of $ZnEt_2$ with acetylacetone (molar ratio 1:1) in toluene resulted in the dimeric complex $[(acac)Zn(Et)]_2$ (**17**) which was used as starting product for **11**. Colorless crystals of compound **17** were obtained from toluene. Due to the insufficient quality of the crystals, only the structure motif could be determined by an X-ray diffraction analysis (Figure 1).

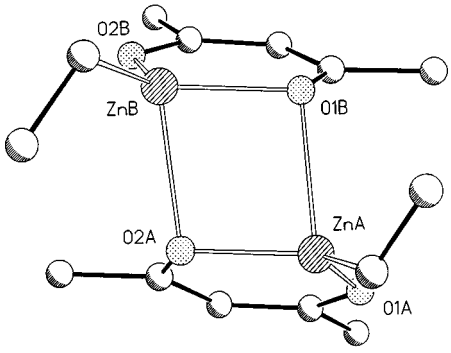

Figure 1. Structure motif of complex **17**

Complex **17** is a dimer in which the two Zn^{II} ions are held together by two bridging oxygen atoms of the acetylacetonate ligands yielding a four-membered Zn_2O_2 ring. Each Zn^{II} centre is tetrahedrally surrounded by three oxygen atoms of the acetylacetonato ligands and one ethyl group. Reaction of **17** with the oxalic amidine in THF (1:1 molar ratio) followed by treatment of the reaction mixture with 1 equiv. $Ni(acac)_2$ resulted in the formation of **11**. Upon recrystallization from toluene, **11** was isolated in 95% purity.

Structures of Dinuclear Complexes

The dinuclear complexes **1**−**11** were characterized by elemental analyses, mass spectrometry, and ^1H and ^{13}C NMR spectroscopy. In addition, the solid-state structures of **1**, **2**, **9**, and **10** were elucidated by X-ray single-crystal diffraction analyses. In principle, dinuclear η^3-allyl complexes containing oxalamidinates with different nitrogen substituents R^1, R^2 can exist in four isomers (Scheme 2), since the oxalamidinato bridge can bind either as the (*E*) isomer or as the

(*Z*) isomer; furthermore, the two η^3-allyl groups can assume *anti* or *syn* positions to each other (Scheme 2, **A**–**D**).

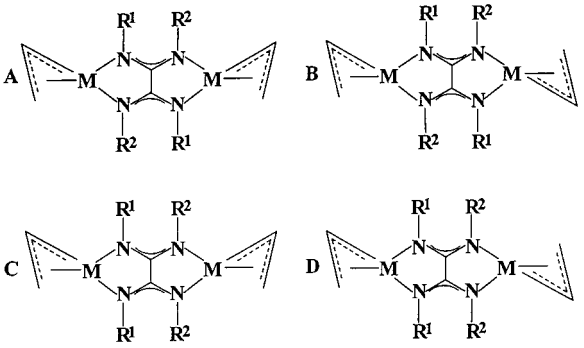

Scheme 2. Possible isomeric allylmetal complexes with bridging oxalamidinato ligands

The mass spectra of the Ni complexes **1** and **2** are typical for dinuclear oxalamidinato allylmetal complexes exhibiting the molecular ion peaks at $m/z = 698$, and 734, respectively, and peaks of smaller fragment ions due to successive loss of the allyl group giving the basic peak, and the (allyl)Ni fragment etc.

Single crystals of complex **1**, grown from *n*-hexane were used to determine its solid-state structure by an X-ray diffraction analysis. The molecular structure of **1** containing an oxalamidinato ligand with two different nitrogen substituents shows that **1** consists of a dimetallic centrosymmetric unit in which the oxalamidinato ligand acts in a bis(chelating) fashion bridging two nickel(II) ions (Figure 2).

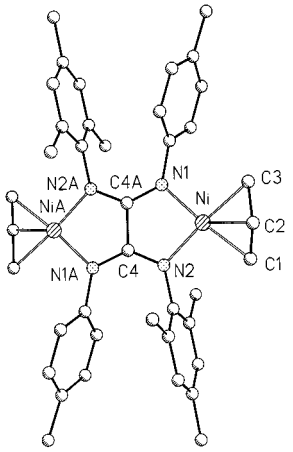

Figure 2. Molecular structure of complex **1**; for clarity the disordered allyl group is omitted; selected bond lengths [Å] and bond angles [°]: Ni–N1 1.912(2), Ni–N2 1.907(2), Ni–C1 1.988(3), Ni–C2 1.970(7), Ni–C3 1.992(3), N1–C4A 1.321(3), N2–C4 1.322(3), C4–C4A 1.522(5); N1–Ni–N2 84.49(9), N1–Ni–C1 174.8(1), N2–Ni–C3 174.0(1), N2–Ni–C1 100.6(1), C1–Ni–C3 73.8(1), Ni–N1–C4A 113.9(2), N1–C4A–C4 113.4(3), C4A–C4–N2 113.2(3), C4–N2–Ni 114.2(2); symmetry transformations used to generated equivalent atoms: A $-x + 1$, $-y + 1$, $-z + 1$

Each metal ion is in a planar environment created by two N atoms from the bridging ligand and the η^3-allyl ligand. The double chelate ring containing the CN_2 units is essentially planar. All C–N bonds are equivalent with a high double-bond character indicating a complete electron delocalization over the two CN_2 units. The C1–C1A bond length between the CN_2 units is that of a single bond [1.522(5) Å]. Other selected bond lengths and angles are listed in Figure 2. The C3, C3A atoms of the allyl groups are disordered and distributed in two positions with equal occupancy factors. Furthermore, the oxalamidinate bridging ligand is coordinated in the (*E*) form. In other words, both isomeric forms **A** and **B** (Scheme 2) are present in the solid state. The Ni–C distances in the allylnickel fragment are identical within the experimental error; furthermore, the aromatic substituents are orientated to the plane of the oxalamidinato bridge at an angle of 82.3 and 78.8°, respectively.

The solid-state structure of complex **2** is very similar to that of **1** (Figure 3). The η^3-allyl groups are also disordered, according to the presence of the *syn* and the *anti* isomer (**A** and **B**, Scheme 2) in the solid state. Bond lengths and angles are very close to those of **1** and need no further discussion.

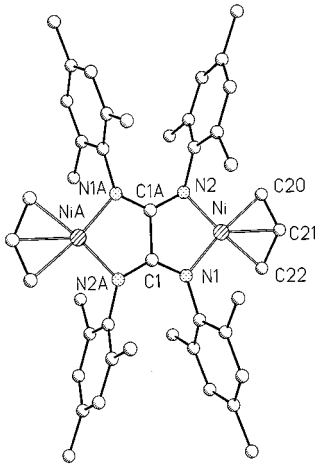

Figure 3. Molecular structure of complex **2**; for clarity the disordered allyl group is omitted; selected bond lengths [Å] and bond angles [°]: Ni–N1 1.919(2), Ni–N2 1.918(2), Ni–C20 2.005(3), Ni–C21 1.986(5), Ni–C22 2.005(3), N1–C1 1.327(3), N2–C1A 1.336(3), C1–C1A 1.525(4); N1–Ni–C20 173.4(1), N1–Ni–N2 85.18(7), N1–Ni–C22 100.5(1), N2–Ni–C20 101.3(1), N2–Ni–C22 174.3(1), C20–Ni–C22 73.1(1), Ni–N1–C1 113.5(1), N1–C1–C1A 114.2(2), C1–C1A–N2 113.3(2), C1A–N2–Ni 113.7(1); symmetry transformations used to generate equivalent atoms: A $-x + 2$, $-y$, $-z + 1$

The NMR-spectroscopic data confirm the presence of both the *syn*- and *anti*-allyl isomers in solution (see Exp. Sect.). The NMR spectra of **2** are relatively complicated. In the ^{1}H NMR spectrum, in [D_8]toluene at room temperature, two doublets of doublets for the CH_2 protons of the terminal allylic group are observed whilst the *meso*-CH protons give a multiplet at $\delta = 5.07$–5.17. These data are in agreement with the existence of two isomers in solution (Scheme 2, **A** and **B**) in which the sterically demanding mesityl groups are unsymmetrically bound giving rise to four different signals for the *o*-mesityl groups as well as for the *p*-methyl groups.

The relatively simple NMR spectra of complex **4** allow a deeper insight into the structure of the complex in $CDCl_3$ solution. In the ^1H NMR spectrum at room temperature only one signal for the protons of the methyl groups of the four *p*-tolyl substituents is observed at δ = 2.06 (relative intensity: 12). The aromatic protons of the CH groups resonate at δ = 6.50 and 6.56. Furthermore, two doublets for the 1-H/1′-H and 2-H/2′-H protons of the allyl groups of C-1 and C-1′, which each integrated for 4 H, are observed.

The most characteristic signals are the resonances of the *meso*-allylic protons, observed at δ = 5.28 and δ = 5.30, both as triplets of triplets integrated for 2 H. This clearly indicates the presence of two isomers in solution, which can be attributed to be the *syn* and the *anti* isomers **A** and **B** (with $R^1 = R^2$, Scheme 2). The molar ratio **A/B** is about 1:1. Consequently, in the ^{13}C NMR spectrum of **4** two resonances for the CH_2 carbon atoms of the allyl groups (at δ = 60.0, and 59.9) are observed. Furthermore, the carbon atoms of the aromatic ring show a double signal set. Additionally, the carbon atoms of the oxalamidinato bridge give rise to two signals at δ = 165.7 and 165.7. This also strongly supports the existence of both **A** and **B** in solution.

The palladium complex **5** contains two different nitrogen substituents and can therefore form four isomers **A**−**D** (Scheme 2). The exact orientation of the nitrogen substituents in the solid state as well as in solution is, however, still unknown.

The solid-state structures of the dinuclear (acetylacetonato)palladium(II) complexes **9** and **10** have also been fully characterized by X-ray diffraction. Figure 4 shows a view of the structure of **9** with the atom-numbering scheme and selected bond lengths and angles.

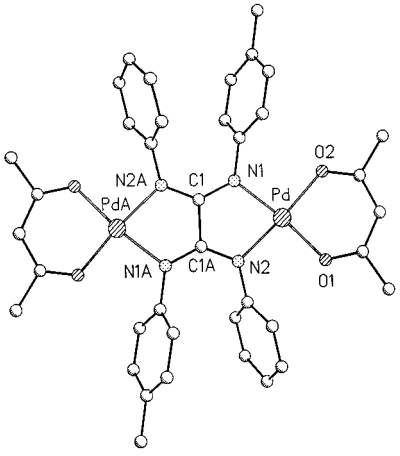

Figure 4. Molecular structure of complex **9**; selected bond lengths [Å] and bond angles [°]: Pd−O1 2.007(2), Pd−O2 2.015(2), Pd−N1 2.015(3), Pd−N2 2.024(3), N1−C1 1.332(4), N2−C1A 1.332(4), C1−C1A 1.522(6); N1−Pd−N2 80.9(1), N1−Pd−O1 173.9(1), N1−Pd−O2 94.3(1), N2−Pd−O1 93.0(1), N2−Pd−O2 174.7(1), O1−Pd−O2 91.79(9), Pd−N1−C1 115.4(2), N1−C1−C1A 114.2(3), C1−C1A−N2 114.5(3), C1A−N2−Pd 115.0(2); symmetry transformations used to generate equivalent atoms: A $-x + 2, -y + 1, -z + 2$

As expected, the coordination around the palladium centre is square-planar. The bond lengths and angles are quite normal and comparable with those of the other dinuclear oxalamidinato complexes. The substituents R^1 and R^2 at the oxalamidinate ligand assume the (*E*) form. In the ^1H NMR spectrum, in $CDCl_3$, complex **9** shows the expected number of resonances for the protons in the aromatic region and for the CH_3 and the CH protons of the acac ligand having the expected intensities.

Complex **10** containing four *p*-tolyl substituents has the same molecular structure in the solid state as **9** (not depicted). Furthermore, the bond lengths and angles are very close to those found in complex **9**. Consequently, the ^1H NMR spectrum of **10** in $[D_8]THF$ at room temperature shows the expected simple pattern for a symmetrical structure: The number of signals of the oxalamidinato and acetylacatonato ligands (δ = 1.43 for the methyl protons of the acac ligand; δ = 2.05 for the *p*-methyl groups; δ = 5.04 for the *meso* proton of acac; δ = 6.52 and 6.59 for the aromatic protons) and their integration confirm the equivalence of the two halves of the complex, as already observed in the solid state. As expected for a symmetrical structure, nine signals were found in the ^{13}C NMR spectrum of **10**.

Tri- and Tetranuclear Complexes Containing Zinc(II) in the Inner Part

The synthesis of oligometal complexes with Zn^{II} as the inner metal ion ("structural" metal) was carried out as follows: According to Scheme 3, 1 equiv. $ZnEt_2$ was very slowly treated with a solution of 2 equiv. of the free oxalamidine. Once the formation of ethane was finished, the in situ formed bis(oxalamidinato)Zn^{II} complex, containing two monoanionic oxalamidinates, was treated with $M(acac)_2$ or with $(allyl)_2Pd$ resulting in the elimination of acetylacetone or propene. Upon workup, the crystalline heterotrinuclear complexes **12**−**14** were isolated (Scheme 3).

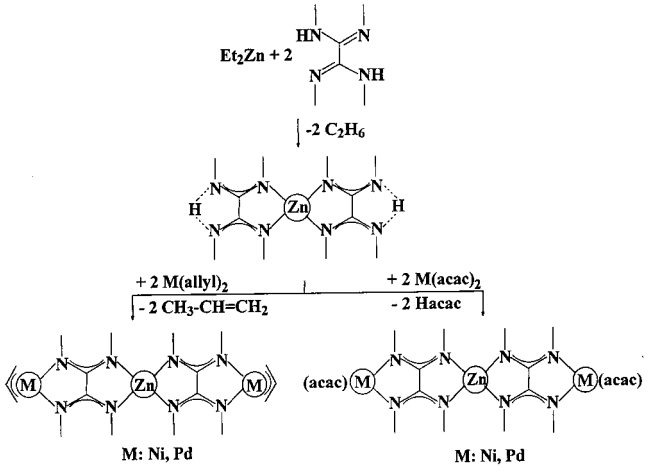

Scheme 3. Formation reaction of the heterotrinuclear complexes **12**−**14** [**12**: Ni(acac), tetramesityloxalic amidinate as bridge; **13**: Pd(acac), tetrakis(*p*-tolyl)oxalic amidinate as bridge; **14**: (allyl)Pd, tetrakis(*p*-tolyl)oxalic amidinate as bridge]

The NMR spectra of **12** and **13** are very similar. Since the Pd complex **13** contains two different types of nitrogen-

bound *p*-tolyl substituents (coordinating either at Pd or at Zn), the ^{1}H NMR spectrum ([D$_8$]THF) displays two resonances at δ = 2.02 and 2.09 for the methyl protons of the *p*-tolyl groups, a singlet for the methyl protons of the acac ligands at δ = 1.54, a singlet for the *meso*-CH group of acac at δ = 5.10, and a multiplet for the aromatic protons between δ = 6.49 and 6.55. The relative intensities of these proton signals (12:12:12:2:32) are in agreement with the trinuclear structure of **13**.

Two different resonances for the methyl protons were also found in the trinuclear η^3-allyl−Pd−Zn−Pd complex **14**. Furthermore, in the region of the CH$_2$ protons of the η^3-allyl groups four signals between δ = 2.66 and 2.44 are observed indicating the presence of two stereoisomers in solution. The ^{13}C NMR spectrum of **14** in CDCl$_3$ at room temperature confirms this. Two signals are indicated for both the carbon atoms of the CH$_2$ group (at δ = 20.52 and 20.58) and the CH group (at δ = 59.9 and 60.5) of the allyl ligands.

The tetranuclear complexes **15** and **16** were formed as follows: In the first step the inner Zn^{II} part was built up in situ by treating 2 equiv. of ZnEt$_2$ with 3 equiv. of the oxalamidine to form a reactive intermediate "[(H-oxam)Zn(oxam)Zn(oxam-H)]", which was able to act as a "metalloligand" using two N−H functions at the periphery for the reaction with 2 equiv. Ni(acac)$_2$. Upon elimination of acetylacetone, **15** crystallized at 0 °C. Alternatively, the above Zn$_2$ intermediate can undergo a reaction with ZnEt$_2$ or [(Et)Zn(acac)]$_2$ (**17**) resulting in the formation of the Zn$_4$ complex **16**.

Both complexes **15** and **16** contain two inner metal ions (Zn) and two peripheral metal ions (Ni or Zn). The single-crystal study of **16** reveals a tetrameric molecule that possesses two acetylacetonate ligands bound to each peripheral Zn ion. The four Zn ions adopt distorted tetrahedral coordination geometries with two ZnN$_4$ donor sets in the middle and two ZnN$_2$O$_2$ donor sets at the periphery. The structure of **16** is depicted in Figure 5. This molecule has no imposed symmetry. The relevant bond lengths and angles are collected in the figure captions. The Zn−N distances of the four Zn-containing tetrahedrons are statistically indistinguishable. Each of the acetylacetonate ligands is bound to Zn in a symmetrical bidentate manner. The Zn(acac) moieties are associated with average Zn−O distances of 1.952(5) Å.

The most interesting finding is, that the bis(mesityl)bis(*p*-tolyl)oxalamidinate ligands coordinate in different forms. The two peripheral oxam ligands assume the (*Z*) configuration with the two mesityl groups situated in peripheral positions. This may be due to the bulkiness of the mesityl groups. In the oxalamidinato bridge in the middle, however, the nitrogen substituents assume the (*E*) configuration. Consequently, the two inner Zn ions are surrounded by three *N*-tolyl groups and one *N*-mesityl group.

The only remarkable difference to the molecular structure of the Ni$_2$Zn$_2$ complex **15** is, that in **15** the peripheral Ni^{II} centres are in a square-planar environment,[10] whereas the inner part adopts the same coordination of the Zn

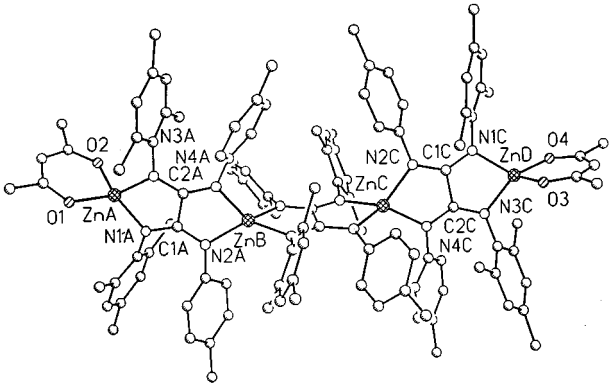

Figure 5. Molecular structure of complex **16**; selected bond lengths [Å] and bond angles [°]: ZnA−O1 1.949(4), ZnA−O2 1.963(5), ZnA−N1A 1.970(5), Zn−N3A 1.990(5), N1A−C1A 1.340(7), N2A−C1A 1.331(7), N3A−C2A 1.338(7), N4A−C2A 1.331(7), C1A−C2A 1.553(9), ZnB−N2A 1.996(5), ZnB−N4A 2.002(5), ZnB−N1B 1.995(5), ZnB−N3B 1.995(5), N1B−C1B 1.324(7), N2B−C1B 1.341(7), N3B−C2B 1.311(7), N4B−C2B 1.347(7), C1B−C2B 1.573(7), ZnC−N2B 1.992(5), ZnC−N4B 1.992(5), ZnC−N2C 2.006(5), ZnC−N4C 1.994(5), N1C−C1C 1.322(8), N2C−C1C 1.341(8), N3C−C2C 1.333(7), N4C−C2C 1.332(8), C1C−C2C 1.571(8), ZnD−N1C 1.978(5), ZnD−N3C 1.986(5), ZnD−O3 1.955(5), ZnD−O4 1.940(5); O1−ZnA−O2 95.3(2), O1−ZnA−N1A 126.1(2), O1−ZnA−N3A 119.7(2), O2−ZnA−N1A 120.6(2), O2−ZnA−N3A 112.7(2), N1A−ZnA−N3A 84.2(2), N2A−ZnB−N4A 83.1(2), N2A−ZnB−N1B 132.0(2), N2A−ZnB−N3B 120.6(2), N4A−ZnB−N1B 121.4(2), N4A−ZnB−N3B 122.6(2), N2B−ZnC−N4B 83.5(2), N2B−ZnC−N2C 120.4(2), N2B−ZnC−N4C 119.4(2), N4B−ZnC−N2C 120.4(2), N4B−ZnC−N4C 133.0(2), N2C−ZnC−N4C 83.1(2), O3−ZnD−O4 95.9(2), O3−ZnD−N1C 115.9(2), O3−ZnD−N3C 117.2(2), O4−ZnD−N1C 123.5(2), O4−ZnD−N3C 122.1(2), N1C−ZnD−N3C 84.4(2)

atoms as in **16**. The relevant bond lengths and angles in **16** are also very close to those in **15**. Since complex **16** has limited solubility in common solvents, its ^{13}C NMR spectrum could not be recorded. The ^{1}H NMR spectrum of **16** consists of six signals for the different methyl groups, one resonance for the CH proton of acac, and the signals for the aryl protons.

Catalytic Reactions

Catalytic Oligomerization/Polymerization of Ethene

Although the catalytic polymerization/oligomerization of ethylene is a well-known reaction[11−13] selective catalysts for the polymerization based on Ni^{II} or other late transition metals are very rare. Recently, Brookhart and co-workers described cationic diimine−Ni and −Pd catalysts as highly active for ethylene polymerization.[14−18] Independently, Brookhart,[19] and Gibson[20] developed cationic Fe^{II} catalysts with tridentate pyridiniminato ligands as efficient catalysts. Very recently, Grubbs and co-workers demonstrated that salicylaldiminatophenyl−Ni^{II} complexes are highly active single-site catalysts for the polymerization of 1-olefins.[21,22] Our initial investigations have shown that some dinuclear (oxalamidinato)Ni^{II} complexes are able to

act as catalysts for the oligomerization or for the polymerization of ethylene.[10]

Here we describe a study of the catalytic behaviour of di- and oligonuclear oxalamidinato complexes towards ethylene with the aim to rationalize the influence of the following three factors: bulkiness of the ligands, nature of the cocatalyst, and effect of the inner metal ion (Zn) on the catalytic activity and selectivity of the peripheral Ni^{II} ions.

The results of ethylene oligomerization/polymerization experiments are listed in Tables 2 and 3, respectively. Several features are noteworthy. In general, the catalysts are moderately active. When the catalytic reactions were carried out under an initial pressure of 10 atm in a sealed autoclave (containing 4000 mol of ethylene per mol catalyst) at 25 °C, the reactions could be used to determine the activities of the catalysts dependent on the above mentioned parameters.

The activities of the catalysts for the oligomerization were calculated from the GC traces, using extrapolated values for C_4-C_8; The catalytic activities for the polymerization were calculated from the amount of the isolated and dried polymer (see Exp. Sect.). Typically, the molecular weights of the polymers formed were around $1.2-6.7 \times 10^5$ g/mol (M_W) with $M_w/M_n = 1.4-2.0$ (Table 2).

Clearly, steric protection of the active sites is a crucial factor in controlling the selectivity and activity (Entries 4−6, Table 2). Upon activation with MAO or Et_3Al complex **8**, containing four sterically demanding mesityl substituents, is a polymerization catalyst. The reduced bulkiness of the four *p*-tolyl substituents on the nitrogen donor atoms in **6** leads to an oligomerization catalyst. In this case only C_4-C_8 olefins, and traces of C_{10} compounds are formed. Complex **7**, possessing both two *p*-tolyl groups and two mesityl groups in a (*Z*) arrangement in the oxam bridge,[10] catalyzes the oligomerization (to form C_4-C_8 olefins) as well as the polymerization reaction (Entry 6, Table 2). From this finding we can conclude that in complex **7** *both* Ni centres are catalytically active: One Ni^{II} centre, surrounded by the bulky mesityl group catalyzes the polymerization of ethylene. The other Ni^{II} centre on the opposite side, coordinating two sterically less demanding nitrogen-bound *p*-tolyl donor groups catalyzes the oligomerization of ethylene to yield C_4-C_8 oligomers.

This conclusion is supported by comparing the catalytic activity of the heterodinuclear Zn−Ni complex **11** with that of the homodinuclear Ni complex **8**. Both **8** and **11** contain

Table 2. Influence of the nitrogen substituents, the nuclearity, and the cocatalyst on the catalytic conversion of ethylene

Entry[a]	Compd.	[Al]/[Ni]	Oligomers C_4	C_6	C_8	Σ oligomers[b] g	TON[c]	Polymer g	TON[c]	M_w	$D = M_w/M_n$
1	**8**	1	−	−	−	−	−	0.13	160	3.57	1.46
2	**8**	3	−	−	−	−	−	0.85	960	4.51	1.49
3	**8**	10	0.06	0.01	−	0.07	80	1.46	1680	4.91	2.66
4	**8**	150	0.20	0.09	−	0.29	340	2.55	2960	1.57	1.78
5	**6**	150	0.83	0.33	0.11	1.27	1470	−	−	−	−
6	**7**	150	0.38	0.16	0.08	0.55	640	0.57	640	2.37	2.02
7[d]	**8**	25	−	−	−	−	−	1.69	1960	−	−
8[d]	**11**	25	−	−	−	−	−	0.86	1000	−	−
9	**12**	150	0.24	−	−	0.24	280	2.83	3280	1.89	1.43
10	**15**	150	0.86	0.40	0.14	1.40	1620	−	−	−	−
11	**8**	1	0.14	−	−	0.14	160	0.90	1040	−	−
12	**8**	2	0.04	−	−	0.04	45	1.06	1240	−	−
13	**8**	3	0.02	−	−	0.02	23	2.14	2480	−	−
14	**8**	10	0.17	0.06	−	0.23	270	2.21	2560	−	−
15	**8**	150	0.18	0.07		0.25	290	2.14	2480	2.46	1.49
16	**6**	150	0.05	0.02	−	0.07	80	−	−	−	−
17	**7**	150	0.03	−	−	0.03	35	−	−	−	−
18	**15**	150	0.03	−	−	0.03	35	−	−	−	−

[a] Solvent: toluene (20 mL); catalysts: 0.031 mmol; ethylene: 0.123 mol in the sealed reactor, ca. 4000 mol ethylene/mol catalyst (ethylene pressure 10 atm); Entries 1−10: MAO as cocatalyst; Entries 11−18: Et_3Al as cocatalyst; reaction time: 16 h (except Entries 7, and 8); reaction temperature 25 °C. − [b] Σ oligomers = g dimers + g trimers + g tetramers (see Exp. Sect.). − [c] TON: turnover number = mol of ethylene consumed/mol of Ni catalyst. − [d] Reaction time 0.5 h.

Table 3. Comparison of the catalytic polymerization of ethylene using **8** and **12** as catalytic precursers: influence of the cocatalyst

Entry[a]	Compd.	Al compd.	Equiv. Al/Ni	h	g polymer	TON[b]
1	**8**	Et_3Al	150:1	1	1.38	1600
2	**12**	Et_3Al	150:1	16	2.51	2920
3	**8**	MAO	150:1	1	2.55	2960
4	**12**	MAO	150:1	16	2.83	3280
5	**8**	Et_3Al	1:1	16	0.90	1040
6	**12**	Et_3Al	1:1	16	2.62	3040
7	**8**	Et_3Al	2:1	16	1.07	1240
8	**12**	Et_3Al	2:1	16	ca. 3.4	ca. 3960
9	**8**	Et_3Al	3:1	16	2.14	2480
10	**12**	Et_3Al	3:1	16	3.00	3480
11	**8**	Et_3Al	150:1	16	2.15	2480
12	**12**	Et_3Al	150:1	16	2.14	2480
13	**8**	Et_2AlCl	150:1	16	2.55	2960

[a] Solvent: toluene (20 mL); catalysts: 0.031 mmol; ethylene: 0.123 mol in the sealed reactor = ca. 4000 mol ethylene/mol catalyst (ethylene pressure: 10 atm); reaction temperature 25 °C. − [b] TON: turnover number = mol of ethylene consumed/mol of Ni catalyst.

four bulky mesityl substituents and therefore act as polymerization catalysts in the presence of MAO. However, **8** contains *two* catalytically active Ni^{II} centres which produce the twofold amount of polyethylene as **11**, in which only *one* Ni^{II} is present while the opposite side of the oxalamidinato bridge is coordinated by Zn^{II} which is inactive (Entries 7 and 8, Table 2).

To examine the role of the cocatalyst in the polymerization we carried out several tests in which the cocatalysts as well as the ratio cocatalyst/Ni were varied. Table 3 lists the results. Upon activation with MAO, **8** is a polymerization catalyst, however a large excess of the cocatalyst is necessary for high turnover numbers (Entry 4, Table 2; Entry 3, Table 3). In contrast, Et_3Al activates the precatalyst **8** which is already at low ratios [Al]/[Ni]: Only 3 equiv. of this cocatalyst per Ni produce an active and selective polymerization catalyst (Entry 9, Table 3) while a large excess does not significantly increase the activity. These results are in agreement with the assumption that in the case of the oxalamidinato complexes bearing dianionic oxalamidinato bridges cationic species are responsible for the catalytic activity. Furthermore, Et_3Al only activates the "polymerization site" of complex **7**, since no oligomerization products were obtained.

To test the influence of the inner metal ion Zn on the catalytic activity we compared the catalytic behavior of the dinuclear complex **8** with that of the trinuclear $ZnNi_2$ complex **12**. Both complexes contain only bulky mesityl substituents and are therefore polymerization catalysts. Table 3 clearly demonstrates that a high excess of MAO ([Al]/[Ni] = 150:1) activates the polymerization of ethylene; however, the Zn-containing complex **12** is significantly more active (Entries 1−4, Table 3). On the other hand, Et_3Al is also a powerful cocatalyst for both complexes; in this case much lower concentrations are required (Entries 5−12, Table 3). The most important finding is, however, that **12** is much more active than **8** when Et_3Al is used. Remarkably, only 2 equiv. Et_3Al per Ni are necessary to establish a highly active system (Entry 8, Table 3). In conclusion, all results of Table 3 clearly demonstrate that the inner Zn ion significantly increases the catalytic activity.

The tetranuclear complex **15** is an oligomerization catalyst, although the two peripheral Ni atoms are surrounded by two bulky *N*-mesityl groups similar to both the catalysts **8** and **12**, which are active in polymerization. The reason for this difference may be seen in the additional influence of the inner coordination polyhedra on the peripheral active Ni^{II} centres. In **8** and **12**, all nitrogen donor groups bear bulky mesityl substituents, while the inner part in **15** contains less bulky *p*-tolyl groups. This difference might be responsible for switching the polymerization activity found for both **8** and **12** to oligomerization activity observed for **15** (Entries 3 and 4, Table 3 versus Entry 18, Table 2). As expected, the Zn_4 complex **16** is catalytically inactive. Furthermore, both the η^3-allyl complexes, and the Pd complexes are inactive.

In order to test the productivity of a typical polymerization catalyst at higher pressure we carried out the catalytic reaction with the system **8**/MAO (1:300) using an initial pressure of 50 bar ethylene at 60 °C. Under these conditions a waxy polymer was formed in a selective polymerization reaction with a turnover frequency of approximately 10^5 mol ethylene consumed/(Ni × h × bar ethylene). This polymer contained about 140 methyl groups per 1000 CH_2 groups, determined by ^1H NMR spectroscopy.

In conclusion, the catalytic activity and selectivity of oligonuclear (oxalamidinato)nickel(II) complexes can be tuned by the bulkiness of the nitrogen substituents (sterically demanding substituents increase the polymerization activity), the nature of the cocatalyst (Et_3Al in low molar ratios is the best cocatalyst), and the nuclearity of the complexes (the inner Zn ion in complexes with bulky nitrogen substituents increases significantly the polymerization activity).

Catalytic Heck Reaction

The Heck coupling is a very useful method for the formation of substituted arylated olefins starting with Ar−X and the substituted olefins, which is catalyzed by a variety of palladium complexes with different controlling ligands.[23,24] Among the most active catalysts are palladacycles with C,P coordination [25−27] and (carbene)palladium complexes.[28−32]

To test the ability for catalyzing the Heck coupling we used, in initial catalytic experiments, some di- and trinuclear palladium complexes as homogeneous catalysts for the coupling of bromoacetophenone with *n*-butyl acrylate. Table 4 shows that most of the coupling reactions were fast and selective, when the catalytic reactions were carried out at 120 °C in dimethylacetamide as solvent using sodium acetate as base. The main product is *n*-butyl (*E*)-4-acetylcinnamate. A deposit of palladium was not observed when the reactions were carried out below 125 °C.

The experimental data clearly show that the influence of different nitrogen substituents is low (Entries 1−4, Table 4). On the other hand, the inner metal ion (Zn) increases the selectivity of the catalytic reaction (Entries 5−8, Table 4). With the heterotrinuclear Pd_2Zn complex **14** turnover numbers of 285000 (after 5 h) and 435000 can be achieved (Entry 8 after 27 h). This corresponds with an average turnover frequency (TOF) of about 57000 mol converted substrate/mol catalyst per hour in the first 5 h and a TOF of about 16100 over the next 27 h. These results clearly demonstrate the catalytic potential of the (oxalamidinato)palladium complexes and give evidence for the activating effects of the inner "structural metal ion" (Zn) on the catalytic behavior of the peripheral "functional" metal ions.

Experimental Section

General: The oxalic amidine ligands were prepared according to literature procedures. CH_3MgBr and CH_3MgCl (3 M in diethyl ether), purchased from Aldrich were used without additional purification. All reactions were carried out under argon and the solvents used were dried by means of standard Schlenk techniques. −

Table 4. Catalytic Heck coupling between bromoacetophenone and *n*-butyl acrylate with di- and trinuclear palladium-based catalysts

Entry[a]	Catalyst	Selectivity (%) [(*E*) product][b]	Conversion (%) 1 h	5 h	22 h	TON 1 h	5 h
1	**3**	92	63	100	100	3150	> 5000
2	**4**	82	64	100	100	3200	> 5000
3	**5**	89	17	70	85	850	> 3500
4	**9**	88	62	100	100	3100	> 5000
5	**13**	96	70	81	85	3500	> 4050
6	**14**	97	64	100	100	3200	> 5000
7	**14**	98	32	70	81	16000	> 35000
8	**14**	96	17	57	85	85000	285000

[a] Conditions: 6.25 mmol *p*-bromoacetophenone, 6.75 mmol *n*-butylacrylate, solvent *N*,*N*-dimethylacetamide (8 mL), 7 mmol CH_3COONa as base, molar ratio substrate/catalyst Entries 1−6: 5000:1; Entry 7: 50000:1; Entry 8: 500000:1; reaction temperature: 120 °C. − [b] *n*-Butyl (*E*)-4-acetylcinnamate.

^1H and ^{13}C NMR spectra were recorded at ambient temperature, unless otherwise stated, with a Bruker AC 200-MHz spectrometer. Numbering for the η^3-allyl groups in the ^1H NMR spectra: CH_2-allyl: 1-H, and 2-H; *meso*-CH-allyl: 3-H. All spectra were referenced to TMS or deuterated solvent as an internal standard. − FAB mass spectra were obtained with a Finnigan MAT SSQ 710 spectrometer (2,4-dimethoxybenzyl alcohol as matrix). − IR measurements were carried out with a Perkin−Elmer System 2000 FT-IR. − Elemental analyses (C, H, and N) were carried out at the Microanalytical Laboratory of the Friedrich-Schiller-Universität Jena. For the determination of the metals, the organic material of the complexes were oxidized using hot concentrated perchloric acid (***CAUTION: Explosions are possible!***) followed by distillation of most of the acid, and slow addition of water to the cold solutions. Metals were determined by complexometric titrations. − The syntheses of the oxalamidinato complexes **6−8**, **11**, and **15** were recently described in a preliminary communication.[10] Oxalic amidines,[33] $(\eta^3\text{-allyl})_2Ni$,[34] and $[\eta^3\text{-allylPdCl}]_2$,[35] were prepared as described. − $(\eta^3\text{-allyl})_2Pd$ was prepared by the following modified method:[36] Bis[(η^3-allyl)chloropalladium(II)] (0.5 g, 1.37 mmol), dissolved in 40 mL of THF, was cooled to −60 °C. To the clear yellow solution allylmagnesium chloride (2.74 mmol of a 2 M solution in THF) was added dropwise under stirring. Then the reaction mixture was allowed to warm very slowly to −30 °C, followed by evaporation of the solvent from the brown solution at −25 °C in vacuo. The solid reaction product was washed twice with 10 mL of *n*-pentane at 18 °C (decomposition at 20 °C), the yellow *n*-pentane solution was cooled to −50 °C. At this temperature the solvent was removed in vacuo.The last step was the sublimation of the reaction product in vacuo at −25 °C to form the very pure complex. Yield 180 mg (70%).

Complex 1: Bis[η^3-allyl(chloro)nickel(II)] (0.263 g, 0.97 mmol) was dissolved in 60 mL of THF. At −78 °C allylmagnesium chloride (1.945 mmol of a 2 M solution in THF) was added very slowly to the stirred solution. Then the yellow reaction mixture was allowed to warm to −20 °C. Slow addition of bis(mesityl)bis(*p*-tolyl)oxalamidine (0.490 g, 0.97 mmol), dissolved in 20 mL of THF, to the stirred solution resulted in a deep yellow solution. After 12 h of stirring at −5 °C, the reaction mixture was warmed to room temperature. After 2 h, the solvent was removed in vacuo. The residue was extracted with *n*-pentane and the solution filtered. At 5 °C yellow crystals of complex **1** formed. Single crystals of **1** were obtained by recrystallization from *n*-pentane or *n*-hexane. Yield 560 mg (82%). − $C_{40}H_{46}N_4Ni_2$ (700.2): calcd. C 68.62, H 6.62, N 8.00, Ni 16.76; found C 68.50, H 6.40, N 7.60, Ni 17.21. − ^1H NMR ([D$_8$]THF, 298 K, 400 MHz): δ = 1.14 (dd, CH_2-allyl, 2 H), 1.35 (dd, CH_2-allyl, 2 H), 1.45 (dd, CH_2-allyl, 2 H), 1.60 (dd, CH_2-allyl, 2 H), 2.00, 2.04 (2 × s, *p*-CH_3 of mesityl, 12 H), 2.16, 2.19, 2.25, 2.27, 2.41, 2.51 (each s, *o*-CH_3 of mesityl, each 3 H), 5.28 (m, CH of allyl, 2 H), 6.47, 6.48 (AA′BB′, CH-tolyl) 6.62 (broad, CH of mesityl, Σ aryl-H = 12 H) − ^{13}C NMR ([D$_8$]THF, 298 K, 100.6 MHz): δ = 18.4, 18.45, 18.54 (*o*-CH_3 of mesityl), 19.7 (2 signals, *p*-CH_3 of tolyl and mesityl), 54.58, 54.60 (CH_2 allyl), 109.9, 110.0, 110.47, 110.53 (CH-allyl), 123.1 (aromatic CH, several signals), 126.9, 127.1, 127.4 (aromatic CH). − IR (nujol): $\tilde{\nu}$ = 1562, 1611 cm^{-1} (C=C_{aromat}, CN). − MS (EI): *m*/*z* (%) = 698 [M^+] (23), 657 [$M^+ - C_3H_5$] (5), 540 [$M^+ - C_3H_6Ni_2$] (0.5), 502 [$M^+ - C_6H_8Ni_2$], 249.42 (basis peak) [$M^+ - C_{37}H_{40}N_4Ni_2$].

Complex 2: The reaction was carried out as described for **1**. Due to the low solubility no ^{13}C NMR spectrum could be obtained. Yield 579 mg (79%). − $C_{44}H_{54}N_4Ni_2$ (757.3): calcd. C 69.88, H 7.20, N 7.41, Ni 15.52; found C 69.22, H 7.81, N 7.1, Ni 14.83. − ^1H NMR ([D$_8$]toluene, 298 K, 200 MHz): δ = 1.34, 1.38, (each dd, CH_2-allyl, 4 H), 1.51, 1.58 (each dd, CH_2-allyl, 4 H), 2.07, 2.08 (2 × s, *p*-CH_3 of mesityl, 12 H), 2.10, 2.11 (2 × s, *p*-CH_3, 12 H) 2.30, 2.39 (2 × s, *o*-CH_3, 12 H, 2.55, 2.64 (2 × s, *o*-CH_3, 12 H), 5.07-5.17 (m, CH of allyl, 2 H), 6.39, 6.41, 6.42, 6.45 (4 × s, CH aromat) − IR (nujol): $\tilde{\nu}$ = 1591, 1613 cm^{-1} (C=C_{aromat}, CN). − MS (EI): *m*/*z* (%) = 754 [M^+] (27), 713 [$M^+ - C_3H_5$] (5), 656 (basis peak) [$M^+ - C_3H_4Ni_2$], 641 [$M^+ - C_6H_8Ni_2$] (42), 614 [$M^+ - C_6H_{10}Ni$].

Complexes 3−5 (General Preparation Procedure): The oxalic amidine (1 mmol) was dissolved in THF and cooled to −30 °C. Then this solution was added at −30 °C to bis([η^3-allyl)palladium(II)] (2.2 mmol in THF). The reaction mixture was allowed to warm to room temperature, followed by distillation of the solvent at −30 °C in vacuo. To remove the excess of bis([η^3-allyl)palladium(II)] the solid was washed three times with 10 mL of *n*-pentane at room temperature.

Complex 3: The crude material was extracted with cyclohexane to remove impurities, washed with *n*-pentane and dried in vacuo. Upon recrystallization from THF yellow crystals were isolated. Yield 640 mg (90%). − $C_{34}H_{34}N_4Pd_2$ (711.5): calcd. C 57.39, H 4.82, N 7.90; found C 56.72, H 4.68, N 7.81. − ^1H NMR (298 K, 200 MHz): δ = 2.04, 2.06 (2 × s, *p*-CH_3, 6 H), 2.51 (m, CH_2-allyl, 8 H), 5.29 (m, CH-allyl, 2 H), 6.56, 6.71 (2 × m, CH aromat, 18 H) − ^{13}C NMR ($CDCl_3$, 298 K, 50.3 MHz): δ = 20.6 (*p*-CH_3), 60.0 (CH_2-allyl), 114.2 (CH-allyl), 121.3, 124.6, 124.9, 127.0, 127.1, 127.4, 127.6, 130.8, 150.2, 152.9 (C-aromat + CH-aromat), 165.74 (C of the oxam bridge). − IR (nujol): $\tilde{\nu}$ = 1591, 1613 cm^{-1} (C=C_{aromat}, CN). − MS (EI): *m*/*z* (%) = 711 [M^+] (4), 563 [$M^+ - C_3H_5Pd$] (1), 418 (2) [$M^+ - C_6H_{10}Pd_2$].

Complex 4: Purification of the crude material was carried out as described for **3**. Yield 629 mg (85%). − $C_{36}H_{38}N_4Pd_2$ (739.5): calcd. C 58.46, H 5.18, N 7.58; found C 58.52, H 5.24, N 7.62. − ^{1}H NMR (298 K, 400 MHz): δ = 2.06 (s, *p*-CH_3, 12 H), 2.45 + 2.47 (d, CH_2-allyl, $^3J_{3,2} = {}^3J_{3',2'}$ = 6.8 Hz, 4 H), 2.56 + 2.58 (d, CH_2-allyl, $^3J_{3,1} = {}^3J_{3',1'}$ = 12.2 Hz, 4 H), 5.28 + 5.30 (2 × tt, *meso*-allyl-CH, $^3J_{1,3} = {}^3J_{1,'3'} = {}^3J_{3',2'}$ = 6.8 Hz, 2 H), 6.50, 6.56 (AA′BB′, CH aromat, $^3J_{AB}$ = 7.8 Hz., 16 H) − ^{13}C NMR ($CDCl_3$, 298 K, 100.6 MHz): δ = 20.6 (*p*-CH_3), 59.95, 59.98 (CH_2-allyl), 114.2 (CH-allyl), 124.47, 124.56, 124.58 (CH aromat), 130.6, 150.26, 150.29 (C-aromat), 165.71, 165.74 (C of the oxam bridge). − IR (nujol): $\tilde{\nu}$ = 1557, 1607, 1639 cm^{-1} (C=C_{aromat}, CN). − MS (EI): *m*/*z* (%) = 738 [M^+] (6), 445 (3) [$M^+ - C_6H_{10}Pd_2$].

Complex 5: The crude material was extracted with diethyl ether at room temperature. Colorless crystals were isolated at 4 °C. Yield 716 mg (90%). − $C_{40}H_{46}N_4Pd_2$ (795.6): calcd. C 60.38, H 5.83, N 7.04; found C 59.68, H 5.51, N 6.84. − ^{1}H NMR ($CDCl_3$, 298 K, 400 MHz): δ = 1.96, 2.01, 2.04, 2.17, 2.19, 2.22, 2.24, 2.25, 2.27, 2.29 (m, CH_3, 24 H), 2.31, 2.33, 2.36, 2.38, 2.44 (m CH_2-allyl, 8 H), 5.22 (m, CH-allyl), 6.32 (broad, CH-aromat, 4 H), 6.48, 6.62 (AA′BB′, $^3J_{AB}$ = 8.1 Hz, CH aromat, 4 H + 4 H). − ^{13}C NMR ([D_8]THF, 298 K, 50.3 MHz): δ = 19.4, 20.6 (CH_3), 57.5, 59.0 (CH_2-allyl), 114.4, 114.5, 114.6 (CH-allyl), 123.5, 123.6, 127.7, 128.2, 128.3 (CH aromat), 129.9, 130.3, 130.4, 131.7, 132.0 (C aromat), 148.8, 150.7 (*ipso*-C of *p*-tolyl, mesityl), 164.4 (C of the oxam bridge). − IR (nujol): $\tilde{\nu}$ = 1539, 155 8, 1609 cm^{-1} (C=C_{aromat}, CN). − MS (EI): *m*/*z* (%) = 794 (31) [M^+], 647 [$M^+ - C_3H_5Pd$].

Complex 9: Bis(phenyl)bis(*p*-tolyl)oxalamidine (418 mg, 1 mmol) and bis(acetylacetonato)palladium(II) 710 mg, 2 mmol), suspended in 20 mL of toluene, were refluxed for 3 h to give a clear solution. Upon distillation of 15 mL of the solvent at normal pressure the solid was filtered from the warm solution and washed first with toluene at room temperature, and then three times with diethyl ether. Recrystallization from hot benzene gave red crystals, suitable for an X-ray analysis. Compound **9** is sparingly soluble in $CHCl_3$, THF, and toluene, and practically insoluble in *n*-pentane. Yield 745 mg (90%). − $C_{38}H_{38}N_4O_4Pd_2$ (827.6): calcd. C 55.15, H 4.63, N 6.77; found C 55.62, H 4.60, N 6.31. − ^{1}H NMR ($CDCl_3$, 298 K, 400 MHz): δ = 1.41, 1.43 (2 × s, CH_3-acac, 12 H), 2.01 (s, CH_3-*p*-tolyl, 6 H), 5.04 (s, CH-acac, 2 H), 6.54−6.60, 6.70 (2 × m, CH-aromat, 16 H). − ^{13}C NMR ([D_8]THF, 298 K, 50.3 MHz): δ = 20.8 (CH_3-*p*-tolyl), 25.2 (CH_3-acac), 100.4 (CH-acac), 123.8, 127.3, 127.4, 128.0, 128.3, 133.4, 142.4, 145.2 (CH-aromat), 169.7 (C, oxam bridge). − IR (nujol): $\tilde{\nu}$ = 1506, 1539, 1578 cm^{-1} (C=C_{aromat}, CN, C=O). − MS (EI): *m*/*z* (%) = 828 (10) [M^+], 728 (4) [M^+ − acac], 621 (1) [M^+ − acacPd], 415 (4) [M+ − $acac_2Pd_2$].

Complex 10: The reaction was carried out as described for **9** using tetrakis(*p*-tolyl)oxalic amidine (440 mg, 0.98 mmol). Yield 755 mg (90%). − $C_{40}H_{42}N_4O_4Pd_2$ (855.6): calcd. C 56.15, H 4.95, N 6.55; found C 55.71, H 4.68, N 6.30. − ^{1}H NMR ($CDCl_3$, 298 K, 400 MHz): δ = 1.43 (s, CH_3-acac, 12 H), 2.05 (s, CH_3-*p*-tolyl, 12 H), 5.04 (s, CH-acac, 2 H), 6.52, 6.59 (AA′BB′, $^3J_{AB}$ = 8.5 Hz, CH-aromat, 12 H). − ^{13}C NMR ($CDCl_3$, 298 K, 50.3 MHz): δ = 20.8 (CH_3-*p*-tolyl), 25.4 (CH_3-acac), 100.3 (CH-acac), 127.1, 127.3, 132.9, 141.4 (CH-aromat), 169.4 (C, oxam bridge), 185.8 (CH-acac). − IR (nujol): $\tilde{\nu}$ = 1506, 1522, 1540, 15744 cm^{-1} (C=C_{aromat}, CN, C=O). − MS (EI): *m*/*z* (%) = 856 (3) [M^+], 756 (4) [M^+ − acac], 657 (4) [M^+ − 2 acac], 649 (3) [M^+ − acacPd], 550 (4) [M^+ − $acac_2Pd$], 443 (7) [M^+ − $acac_2Pd_2$].

Complex 12: Tetramesityloxalic amidine (2 mmol, 1.12 g) was dissolved in 50 mL of THF, and dropwise treated with $ZnEt_2$ (1.1 M solution in toluene, 0.91 mL) at room temperature. After stirring and heating for about 30 min, a solution of bis(acetylacetonato)-nickel(II) (0.51 g, 2 mmol in 10 mL of THF) was added. The color turned red within a few minutes. After stirring overnight, a red microcrystalline substance precipitated. The precipitate was filtered and washed with 10 mL of diethyl ether. Yield about 0.90 g (30%). − $C_{86}H_{102}N_8Ni_2O_4Zn$ (1494.6): calcd. C 69.11, H 6.88, N 7.50, Ni 7.85, Zn 4.38; found C 69.42, H 6.51, N 7.20, Ni 7.24, Zn 4.23. − ^{1}H NMR ([D_8]THF, 298 K, 200 MHz): δ = 1.05, 1.13 (m, CH_3-acac, 12 H), 1.69 (s, CH_3-mesityl, 12 H), 1.93, 1.95 (s, CH_3-mesityl, 12 H), 2.14 (s, CH_3-mesityl, 12 H), 2.50, 2.53, (s, CH_3-mesityl, 36 H), 4.98, 5.05 (s, CH-acac, 2 H), 6.25−6.34 (m, CH-aromat, 16 H). − ^{13}C NMR ([D_8]THF, 298 K, 50.3 MHz): δ = 19.7, 20.5, 20.6, 21.0 (CH_3-aromat), 24.9 (CH_3-acac), 100.3, 100.7 (CH-acac), 127.7, 127.9, 128.4, 131.9, 132.3, 132.9, 133.1, 134.55, 134.63, 140.64, 141.3, 143.1 (C-aromat), 162.6, 166.4 (C_{tert}-bridge), 186.8, 194.6 (CO-acac).

Complex 13: To a stirred solution of tetrakis(*p*-tolyl)oxalic amidine (440 mg, 0.98 mmol) in 30 mL of toluene, $ZnEt_2$ (0.49 mmol), dissolved in 20 mL of toluene, was slowly added dropwise, followed by 15 min of stirring. At room temperature a suspension of bis(acetylacetonato)palladium(II) (300 mg, 0.98 mmol) in 20 mL of toluene was added and the mixture was refluxed for 1 h. The solvent was then removed in vacuo, and the orange residue was washed four times with 10-mL portions of *n*-pentane. The residue was dissolved in 50 mL of diethyl ether under 15 min of stirring and filtered. The solvent was very slowly removed. In a first fraction Pd(acac)$_2$ crystallized from the solution, while **15** crystallized later. Upon dissolution of impure **15** in diethyl ether this procedure was repeated. Orange crystals of **15** were isolated, which are soluble in THF, toluene, and diethyl ether, and practically insoluble in *n*-pentane. Yield 602 mg (45%). − $C_{70}H_{70}N_8O_4Pd_2Zn$ (1365.6): calcd. C 61.57, H 5.17, N 8.21; found C 61.3, H 5.22, N 7.66. − ^{1}H NMR ($CDCl_3$, 298 K, 400 MHz): δ = 1.54 (s, CH_3-acac, 12 H), 2.09, 2.20 (2 × s, CH_3-*p*-tolyl, 24 H), 5.10 (s, CH-acac, 2 H), 6.25−6.55 (m CH-aromat, 32 H). − ^{13}C NMR ($CDCl_3$, 298 K, 50.3 MHz): δ = 20.7, 20.8 (CH_3-*p*-tolyl), 24.6 (CH_3-acac), 100.4 (CH-acac), (CH-aromat), 162.1 (C, oxam bridge), 186.4 (CH-acac). − IR (nujol): $\tilde{\nu}$ = 1507, 1540, 1572, 110 cm^{-1} (C=C_{aromat}, CN, C=O). − MS (ESI, THF/CH_3OH/$CHCl_3$ as solvent mixture): *m*/*z* (%) = 1159 (1) [M^+ − acacPd], 475 (100) [M^+ − $acac_2Pd_2$], 444 [M^+ − $acac_2Pd_2$ − Zn].

Complex 14: The reaction was carried out as described for **13** using bis([η^3-allyl)palladium(II)] at 0 °C. Upon distillation of the solvent in vacuo the residue was washed four times with *n*-pentane. Recrystallization from diethyl ether yielded yellow crystals soluble in THF, toluene, and diethyl ether. Compound **14** contains 1 equiv. diethyl ether/mol complex (GC). Yield 480 mg (36%). − $C_{70}H_{76}N_8OPd_2Zn$ (1323.6): calcd. C 63.35, H 5.74, N 8.47, Zn 4.94; found C 63.73, H 5.60, N 8.21, Zn 4.70. − ^{1}H NMR ($CDCl_3$, 298 K, 200 MHz): δ = 2.03, 2.06 (s, CH_3-*p*-tolyl, 24 H), 2.44, 2.47, 2.54 (3 × d, CH_2-allyl, $^3J_{3,2}$ = 3.4 Hz, 3 H), 2.66 (m, CH_2-allyl, 5 H), 5.31 (m, CH-allyl, 2 H), 6.16−6.51 (m, CH-aromat, 32 H). − ^{13}C NMR ($CDCl_3$, 298 K, 50.3 MHz): δ = 20.52, 20.58 (CH_3-*p*-tolyl), 59.9, 60.5 (CH_2-allyl) 114.1, 114.3 (CH-allyl), 123.97, 123.01, 124.2, 124.6, 127.47, 127.51, 127.66, 127.71, 130.48, 130.51, 130.99, 131.02 (CH-aromat), 143.77, 143.82, 150.0, 150.3 (C-aromat), 160.7, 160.8 (C oxam bridge). − IR (nujol): $\tilde{\nu}$ = 1506, 1609 cm^{-1} (C=C_{aromat}, CN). − MS (EI): *m*/*z* (%) = 1248 (< 1) [M^+], 740 (5) [M^+ − oxamZn], 591 (2) [M^+ − allylPd − oxamZn].

Complex 16: Bis(mesityl)bis(*p*-tolyl)oxalic amidine (1 mmol, 0.50 g) was dissolved in 38 mL of THF, and treated dropwise with 2 mmol

of $ZnEt_2$ (1.1 M solution in toluene, 1.8 mL) at room temperature. After 5 min of heating, the solution was stirred for 20 min and then treated with bis(mesityl)bis(*p*-tolyl)oxalic amidine (2 mmol, 1.0 g, dissolved in 12 mL of THF). This solution was refluxed for 3 min, cooled and treated with bis(acetylacetonato)(ethyl)zink(II) complex **19** (2 mmol, 0.387 g, dissolved in 10 mL of THF). Standing at room temperature for 2 d resulted in the crystallization of pure, colorless crystals of **16**, crystallizing with 2.5 equiv. THF, suitable for an X-ray analysis. Yield 290 mg (45%). − $C_{112}H_{122}N_{12}O_4Zn_4 \times 2.5$ C_4H_8O (2142.1): calcd. C 68.41, H 6.68, N 7.85; found C 67.0 H, 6.55, N 7.42. − ^{1}H NMR ($CDCl_3$, 298 K, 400 MHz): δ = 1.49, 1.64, 1.77, 1.91, 2.01, 2.08 (s, CH_3-acac, CH_3-*p*-tolyl, CH_3-mesityl, 84 H), 5.01 (s, CH-acac, 2 H), 6.1−6.54 (CH-aromat, 36 H). − MS (ESI in CH_3OH/THF): *m*/*z* (%) = 1067 (4) [$Zn(oxam)_2$].

Complex 17: Acetylacetone (10 mmol, 1.001 g), dissolved in 10 mL of toluene, was slowly treated with $ZnEt_2$ (10 mmol, 1.1 M toluene solution) at room temperature. After all the ethane was released, the solution was kept at −18 °C and colorless crystals were isolated. Yield 2.11 g (55%). − $C_{14}H_{24}O_4Zn_2$ (387.1): calcd. C 43.43, H 6.25; found C 43.64, H 6.11. − ^{1}H NMR ([D_8]toluene, 298 K, 200 MHz): δ = 0.52 (q, CH_2-ethyl, 2 H), 1.44 (t, CH_3-ethyl, 3 H), 1.75 (s, CH_3-acac, 6 H), 5.01 (s CH-acac 1 H). − ^{13}C NMR ([D_8]toluene, 298 K, 50.3 MHz): δ = − 0.03 (CH_2-ethyl), 12.8 (CH_3-methyl), 28.1 (CH_3-acac), 101.8 (CH-acac). − MS (EI): *m*/*z* (%) = 262 (61) [$Zn(acac)_2$], 192 (6) [M^+/2], 163 (68) [M^+/2 − 2 Et].

Catalytic Polymerization/Oligomerization: A 200-mL stainless steel autoclave was heated in vacuo for 2 h at approximately 100 °C and subsequently cooled to 25 °C. A solution of 0.031 mol of the catalyst precursor, dissolved in toluene, was treated either with MAO (5 M solution in toluene) or with Et_3Al (1.9 M solution in toluene). The total volume of the added solutions was 20 mL. After the autoclave was charged with this solution, catalytic reactions were carried out at 25 °C in the sealed autoclave whilst stirring (initial pressure of ethylene: 10 atm = 0.123 mol ethylene). No further ethylene was added during the reaction. After the desired reaction time (Tables 2 and 3) the reaction mixture was cooled to 0 °C. The ethylene pressure was then released, and the cooled reaction mixture was treated with a small amount of dilute hydrochloric acid at 0 °C to inactivate the catalyst, followed by addition of 1.18 mL (0.87 g) of *n*-decane as standard for GC measurements.

Analysis of the Ethylene Oligomers: An aliquot (1 mL) of the reaction mixture was very slowly treated with dilute hydrochloric acid at 0 °C, followed by separation of the organic layer. After drying the organic phase with solid Na_2CO_3, the oligomers were analyzed by GC/MS using a methylsilicon column (CPSIL 5 CB), injector temperature 40 °C, with the following temperature program: 20 °C/min up to 300 °C (15 min). The individual products were identified by MS and integrated, using *n*-decane as the internal standard (comparison with GC calibration experiments). The turnover numbers (TON) were calculated as follows:

mol ethylene consumed = g oligomers/mol weight of ethylene = g oligomers/28 $gmol^{-1}$

TON = mol of ethylene consumed/mol catalyst = mol of ethylene consumed/$0.031 \cdot 10^{-3}$ mol catalyst.

In a typical example the following C_6 olefins from the catalysis with the oligomerization catalyst **6** (Entry 5, Table 2) were characterized by GC/IR (comparison with authentic samples): overall amount of C_6 olefins = 0.33 g (100%); 4-methylpentene: 2.1%; 2,3-dimethylbutene 3.2%; 1-hexene: 53%; *trans*-3-hexene: 21%; *trans*-2-hexene: 3.2%. Retention times under the analytical conditions used were as follows: butenes: 1.238 min; 4-methylpentene: 1.478 min; 2,3-dimethylbutene: 1.584 min; 1-hexene: 1.644 min; *trans*-3-hexene: 1.69 min; *trans*-2-hexene: 1.72 min. − In most of the catalytic reactions (Tables 2 and 3) only C_4 and C_6 olefins were found. Small amounts of C_8 olefins were found in a few of the catalytic reactions (Entries 5, 6, and 10, Table 2). C_{10} oligomers were detected only in traces (Entry 5, Table 2).

Analysis of the Polymer: An aliquot of the above solution was treated with a mixture of 500 mL of methanol and 20 mL of hydrochloric acid while stirring to precipitate the polymer. After the methanol/hydrochloric acid mixture was decanted, the polymer was washed with methanol (3 × 50 mL), and dried at 70 °C in vacuo. Yields and molecular weights can be found in Tables 2 and 3. The TONs for the polymerization were determined analogously with the above calculation (see Tables 2 and 3). The polymers were analyzed by GPC using THF as a solvent and polystyrene standards. Columns were packed with styrene−divinylbenzene copolymer; column temperature: 30 °C; flow rate: 1.00 mL/min; detector 1: UV 975 (Fa. Jasco); detector 2: RI 930 (Fa. Jasco). − Typically, M_w was around $1.57 \cdot 10^5$ to $6.73 \cdot 10^5$ with polydispersity indices between 1.46 and 2.66 (Table 2).

Polymerization at Higher Pressure: A typical experiment proceeded as follows: 0.031 mmol of complex **8** and $0.93 \cdot 10^{-2}$ mol of MAO ([Ni]/[Al] = 1:150) were dissolved in 20 mL of toluene. The catalysis was carried out at 55 bar ethylene pressure at 60 °C and stirring of the reaction mixture for 10 min. The isolation of the polymer followed the above procedure. Yield 9.1 g; turnover frequency (TOF): approximately 55 g/mmol cat × bar × h. In this case a waxy polymer was obtained. According to the integration of the CH, CH_2, and CH_3 protons in the ^{1}H NMR spectrum ([D_8]toluene, 298 K, 200 MHz) approximately 140 branches/1000 ethylene units were present.

Heck Coupling: In a typical run, a 25-mL Schlenk tube was charged with an aryl halide (6.25 mmol), anhydrous sodium acetate (7 mmol) and put under argon followed by addition of *N*,*N*-dimethylacetamide (8 mL) and *n*-butyl acrylate (6.75 mmol) The solution was heated to 120 °C before the catalyst, dissolved in toluene, was added. After the reaction time, the reaction mixture was cooled and analyzed by gas chromatography.

Crystal Structure Determination: The intensity data for the compounds were collected with a Nonius KappaCCD diffractometer, using graphite-monochromated Mo-K_α radiation. Data were corrected for Lorentz and polarization effects, but not for absorption.[37,38] The structures were solved by direct methods (SHELXS[39]) and refined by full-matrix least-squares techniques against F_o^2 (SHELXL-97[40]). Since the quality of the data of compound **17** is too bad, only the conformation of the molecule and the crystallographic data are communicated. Furthermore, this data will not be published in the Cambridge Crystallographic Data Centre. The allyl groups of **1** and **2** are disordered. The disorder could be solved. The hydrogen atoms were included at calculated positions with fixed thermal parameters. All non-hydrogen atoms were refined anisotropically.[41] XP (SIEMENS Analytical X-ray Instruments, Inc.) was used for structure representations.

Crystal Data for 1:[41] $C_{40}H_{46}N_4Ni_2$, M_r = 700.23 g·mol^{-1}, gold-yellow prism, size 0.20 × 0.20 × 0.10 mm, triclinic, space group $P\bar{1}$, *a* = 8.8877(4), *b* = 9.2005(5), *c* = 11.8562(5) Å, α = 107.550(3), β = 95.843(3), γ = 98.779(3)°, *V* = 902.23(7) Å^3, *T* = −90 °C, *Z* = 1, $\rho_{calcd.}$ = 1.289 gcm^{-3}, μ(Mo-K_α) = 10.76 cm^{-1}, *F*(000) = 370, 6624 reflections in *h*(−11/11), *k*(−11/11), *l*(−15/14), measured in the range 3.19° ≤ Θ ≤ 27.53°, completeness Θ_{max} = 98.7%, 4104 independent reflections, R_{int} = 0.028, 3353 reflections with $F_o > 4\sigma(F_o)$, 218 parameters, 0 restraints, $R1_{obs}$ = 0.053, wR^2_{obs} = 0.101,

$R1_{all}$ = 0.075, wR^2_{all} = 0.108, GOOF = 1.073, largest difference peak and hole: 0.388/−0.358 e·Å^{-3}.

Crystal Data for 2:[41] $C_{44}H_{54}N_4Ni_2$, M_r = 757.33 g·mol^{-1}, gold-yellow prism, size 0.20 × 0.20 × 0.08 mm, triclinic, space group $P\bar{1}$, a = 8.4970(3), b = 10.5059(6), c = 12.4798(6) Å, α = 65.704(2), β = 87.798(3), γ = 76.103(3)°, V = 983.36(8) Å^3, T = −90 °C, Z = 1, $\rho_{calcd.}$ = 1.277 gcm^{-3}, μ(Mo-K_α) = 9.92 cm^{-1}, F(000) = 370, 7625 reflections in h(−11/11), k(−13/13), l(−16/16), measured in the range 4.33° ≤ Θ ≤ 27.49°, completeness Θ_{max} = 98.4%, 4442 independent reflections, R_{int} = 0.038, 3592 reflections with $F_o > 4\sigma(F_o)$, 300 parameters, 0 restraints, $R1_{obs}$ = 0.043, wR^2_{obs} = 0.091, $R1_{all}$ = 0.063, wR^2_{all} = 0.098, GOOF = 1.025, largest difference peak and hole: 0.357/−0.341 e·Å^{-3}.

Crystal Data for 9:[41] $C_{38}H_{38}N_4O_4Pd_2$, M_r = 827.62 g·mol^{-1}, light yellow prism, size 0.20 × 0.18 × 0.12 mm, monoclinic, space group $P2_1/c$, a = 12.5830(4), b = 8.8054(5), c = 15.9510(9) Å, β = 91.319(3)°, V = 1766.9(1) Å^3, T = −90 °C, Z = 2, $\rho_{calcd.}$ = 1.555 gcm^{-3}, μ(Mo-K_α) = 10.63 cm^{-1}, F(000) = 836, 12946 reflections in h(−16/14), k(−11/10), l(−20/17), measured in the range 3.45° ≤ Θ ≤ 27.51°, completeness Θ_{max} = 98.4%, 3996 independent reflections, R_{int} = 0.051, 3228 reflections with $F_o > 4\sigma(F_o)$, 226 parameters, 0 restraints, $R1_{obs}$ = 0.041, wR^2_{obs} = 0.086, $R1_{all}$ = 0.061, wR^2_{all} = 0.092, GOOF = 1.030, largest difference peak and hole: 0.526/−0.904 e·Å^{-3}.

Crystal Data for 10:[41] $C_{40}H_{42}N_4O_4Pd_2$, M_r = 855.58 gmol^{-1}, light yellow prism, size 0.12 × 0.12 × 0.10 mm, monoclinic, space group $P2_1/c$, a = 12.6868(9), b = 8.7318(6), c = 16.393(1) Å, β = 92.982(4)°, V = 1813.5(2) Å^3, T = −90 °C, Z = 2, $\rho_{calcd.}$ = 1.567 gcm^{-3}, μ(Mo-K_α) = 10.38 cm^{-1}, F(000) = 868, 11592 reflections in h(−16/14), k(−11/10), l(−21/16), measured in the range 3.13° ≤ Θ ≤ 27.50°, completeness Θ_{max} = 99.1%, 4126 independent reflections, R_{int} = 0.087, 2828 reflections with $F_o > 4\sigma(F_o)$, 226 parameters, 0 restraints, $R1_{obs}$ = 0.062, wR^2_{obs} = 0.105, $R1_{all}$ = 0.108, wR^2_{all} = 0.119, GOOF = 1.024, largest difference peak and hole: 1.126/−0.797 e·Å^{-3}.

Crystal Data for 16:[41] $C_{112}H_{122}N_{12}O_4\ Zn_4 \times 2.5\ C_4H_8O$, M_r = 2142.1 g·mol^{-1}, colourless prism, size 0.24 × 0.22 × 0.10 mm, triclinic, space group $P\bar{1}$, a = 16.7787(5), b = 16.9800(5), c = 23.1886(7) Å, α = 102.894(2), β = 98.691(2), γ = 105.365(2)°, V = 6052.4(3) Å^3, T = −90 °C, Z = 2, $\rho_{calcd.}$ = 1.171 gcm^{-3}, μ(Mo-K_α) = 8.38 cm^{-1}, F(000) = 2244, 45031 reflections in h(−21/19), k(−21/22), l(−30/30), measured in the range 2.98° ≤ Θ ≤ 27.51°, completeness Θ_{max} = 98.6%, 27436 independent reflections, R_{int} = 0.088, 16443 reflections with $F_o > 4\sigma(F_o)$, 1237 parameters, 0 restraints, $R1_{obs}$ = 0.111, wR^2_{obs} = 0.224, $R1_{all}$ = 0.187, wR^2_{all} = 0.259, GOOF = 1.080, largest difference peak and hole: 1.220/−0.995 e·Å^{-3}.

Crystal Data for 17: $C_{14}H_{24}O_4Zn_2$, M_r = 387.07 g·mol^{-1}, colourless prism, size 0.32 × 0.30 × 0.28 mm, orthorhombic, space group $Pbca$, a = 12.795(2), b = 15.865(2), c = 17.637(3) Å, V = 3580.2(9) Å^3, T = −90 °C, Z = 8, $\rho_{calcd.}$ = 1.436 gcm^{-3}, μ(Mo-K_α) = 26.87 cm^{-1}, F(000) = 1600, 10076 reflections in h(−16/16), k(−20/20), l(−22/22), measured in the range 3.09° ≤ Θ ≤ 27.43°, completeness Θ_{max} = 94.1%, 3853 independent reflections, R_{int} = 0.182.

Acknowledgments

Financial support for this work from the Deutsche Forschungsgemeinschaft, the VW-Stiftung and the Fonds der Chemischen Industrie is gratefully acknowledged.

[1] W. E. Hofman, *Proc. Indiana Acad. Sci.* **1969**, *79*, 129; *Chem. Abstr.* **1970**, *73*, 126513r.
[2] E. Papavil, *Anal. Stiint. Univ. Jasi, Sect. 110* **1964**, 115; *Chem. Abstr.* **1965**, *63*, 14351h.
[3] M. Pasquali, C. Floriani, A. Chiesi-Villa, C. Guastini, *J. Am. Chem. Soc.* **1979**, *101*, 4740.
[4] P. Fehling, M. Döring, F. Knoch, R. Beckert, H. Görls, *Chem. Ber.* **1995**, *128*, 405.
[5] M. Döring, H. Görls, R. Beckert, *Z. Anorg. Allg. Chem.* **1994**, *620*, 551.
[6] R. Beckert, S. Vorwerk, D. Lindauer, M. Döring, *Z. Naturforsch., Teil B* **1993**, *48*, 1186.
[7] M. Döring, P. Fehling, H. Görls, W. Imhof, R. Beckert, D. Lindauer, *J. Prakt. Chem.* **1999**, *341*, 748.
[8] M. Ruben, S. Rau, A. Skirl, K. Krause, H. Görls, D. Walther, J. G. Vos, *Inorg. Chim. Acta* **2000**, *303*, 206
[9] M. Ruben, D. Walther, R. Knake, H. Görls, R. Beckert, *Eur. J. Inorg. Chem.* **2000**, 1055.
[10] T. Döhler, H. Görls, D. Walther, *Chem. Commun.* **2000**, 945.
[11] For recent reviews see: G. J. P. Britovsek, V. C. Gibson, *Angew. Chem.* **1999**, *111*, 448; *Angew. Chem. Int. Ed.* **1999**, *38*, 428.
[12] K. A. O. Starzewski, W. M. Kelly, A. Stump, D. Freitag, *Angew. Chem.* **1999**, *111*, 2588; *Angew. Chem. Int. Ed.* **1998**, *38*, 2439.
[13] H. H. Brintzinger, D. Fischer, R. Mühlhaupt, B. Rieger, R. M. Waymouth, *Angew. Chem.* **1995**, *107*, 1255; *Angew. Chem. Int. Ed. Engl.* **1995**, *34*, 1143.
[14] L. K. Johnson, C. M. Killian, S. D. Arthur, J. Feldman, E. F. McCord, S. J. McLain, K. Kreutzer, M. A. Bennett, E. B. Coughlin, S. D. Ittel, A. Parthasarathy, D. J. Tempel, M. S. Brookhart (DuPont), WO-A 96/231010, **1996** [*Chem. Abstr.* **1996**, *125*, 222773t].
[15] L. K. Johnson, C. M. Killian, M. S. Brookhart, *J. Am. Chem. Soc.* **1995**, *117*, 6414.
[16] C. M. Killian, D. J. Tempel, L. K. Johnson, M. S. Brookhart, *J. Am. Chem. Soc.* **1996**, *118*, 11664.
[17] S. Mecking, L. K. Johnson, M. Brookhart, *J. Am. Chem. Soc.* **1996**, *118*, 267.
[18] S. Mecking, L. K. Johnson, L. Wang, M. Brookhart, *J. Am. Chem. Soc.* **1998**, *120*, 888.
[19] B. L. Small, M. Brookhart, A. M. A. Bennett, *J. Am. Chem. Soc.* **1998**, *120*, 4049.
[20] G. J. P. Britovsek, V. C. Gibson, B. S. Kimberley, P. J. Maddox, S. J. McTauish, G. A. Solan, A. J. P. White, D. J. Williams, *Chem. Commun.* **1998**, 849.
[21] T. R. Younkin, E. F. Connor, J. I. Henderson, S. K. Friedrich, R. H. Grubbs, D. A. Bansleben, *Science* **2000**, *287*, 460.
[22] C. Wang, S. Friedrich, T. R. Younkin, R. T. Li, R. H. Grubbs, D. A. Bansleben, M. W. Day, *Organometallics* **1998**, *17*, 3149.
[23] A. de Meijere, F. Meyer, *Angew. Chem.* **1994**, *106*, 2473; *Angew. Chem. Int. Ed. Engl.* **1994**, *33*, 2379.
[24] V. V. Grushin, H. Alper, *Chem. Rev.* **1994**, *106*, 2473; W. Cabri, I. Caudiani, *Acc. Chem. Res.* **1995**, *28*, 2.
[25] W. A. Herrmann, C. Broßmer, K. Öfele, C.-P. Reisinger, T. Priermeier, M. Beller, H. Fischer, *Angew. Chem.* **1995**, *107*, 1989; *Angew. Chem. Int. Ed. Engl.* **1995**, *28*, 1844.
[26] W. A. Herrmann, V. Böhm, *J. Organomet. Chem.* **1999**, *572*, 141.
[27] W. A. Herrmann, V. Böhm, C.-P. Reisinger, *J. Organomet. Chem.* **1999**, *576*, 23.
[28] W. A. Herrmann, M. Elison, J. Fischer, C. Köcher, G. R. J. Artus, *Angew. Chem.* **1995**, *107*, 2602; *Angew. Chem. Int. Ed. Engl.* **1995**, *34*, 2371.
[29] W. A. Herrmann, C.-P. Reisinger, M. J. Spiegler, *J. Organomet. Chem.* **1998**, *557*, 93.
[30] W. A. Herrmann, Th. Weskamp, V. P. W. Böhm, *J. Organomet. Chem.* **1999**, *585*, 348.
[31] W. A. Herrmann, V. Böhm, *Chem. Eur. J.* **2000**, *6*, 1017.
[32] D. S. McGuiness, K. J. Cavell, *Organometallics* **2000**, *19*, 741.

[33] R. Bauer, *Ber. Dtsch. Chem. Ges.* **1907**, *40*, 2650.
[34] G. Wilke, B. Bogdanovic, *Angew. Chem.* **1961**, *23*, 756.
[35] J. Smidt, W. Hafner, *Angew. Chem.* **1959**, *71*, 284.
[36] G. Wilke, Belg. Patent, **1963**, 631172.
[37] COLLECT, Data Collection Software, Nonius B. V., Netherlands, **1998**.
[38] Z. Otwinowski, W. Minor, *Processing of X-ray Diffraction Data Collected in Oscillation Mode*, in: *Methods in Enzymology*, vol. 276, Macromolecular Crystallography, Part A (Ed.: C. W. Carter, R. M. Sweet), pp. 307−326, Academic Press, San Diego, **1997**.
[39] G. M. Sheldrick, *Acta Crystallogr., Sect. A* **1990**, *46*, 467−473.
[40] G. M. Sheldrick, *SHELXL-97*, University of Göttingen, Germany, **1993**.
[41] Further details of the crystal structure investigations are available on requests from the Cambridge Crystallographic Data Centre, 12 Union Road, Cambridge CB2 1 EZ, UK, on quoting the depository numbers CCSD-152478 (**1**), -152482 (**2**), -152479 (**9**), -152480 (**10**), and -152481 (**16**), the names of the authors, and the journal citation.

Received December 6, 2000
[I00464]